Int J Adv Manuf Technol (2014) 72:1513–1525
DOI 10.1007/s00170-014-5695-9

ORIGINAL ARTICLE

A study on the effect of rectangular cut out on laser forming of AISI 304 plates

K. Paramasivan · Sandip Das · Dipten Misra

Received: 8 August 2013 / Accepted: 6 February 2014 / Published online: 23 March 2014

Abstract Laser bending of a rectangular AISI 304 plate with a rectangular cut out is investigated in the present work. In particular, effects of process parameters: laser power, scanning speed, and geometric parameters: dimensions of the cut out of sheet metal on temperature distribution and bending angle are explored with the help of numerical simulation. Analyses are carried out through a coupled thermo-mechanical formulation with finite element method using COMSOL MULTIPHYSICS. The temperature distribution and deformation of sheet metal have been obtained from numerical simulations. The bending angle is affected by process parameters, namely, laser power, scanning speed, and width of the cut out of the sheet metal. Position of the cut out vis-à-vis the scanning path and length of the cut out have very little effect on the bending angle.

Keywords Laser forming · Finite element analysis · Rectangular cut out · Bending angle

1 Introduction

Laser forming is realized by introducing residual thermal stresses in the component under consideration. These internal stresses induce plastic strains to generate a bend angle in the components. Presently, laser forming process is employed in diverse industries, such as aerospace, automotive, microelectronics, and shipbuilding that had previously relied on expensive dies and presses for prototype evaluations. In contrast to conventional forming techniques, this method requires no mechanical contact and possesses the inherent advantage of process flexibility associated with laser manufacturing techniques.

Till date, a large number of studies have been carried out in the area of laser forming and associated numerical techniques. Shen and Vollertsen [1] investigated the modeling strategies of laser forming. The temperature field during laser forming is simulated by Ji and Wu [2]. In their following work, Wu and Ji [3] presented the deformation field during laser forming of sheet metal. Shi et al. [4] studied the temperature gradient mechanism (TGM) to achieve high accuracy forming. Venkadeshwaran et al. [5] studied the deformation field in circular plate by using circle line heating. Yu et al. [6] developed a finite element model (FEM) for thermo-mechanical analysis of metal plate forming. They have shown the importance of refinement of mesh density on temperature distribution and final distortion. Zohoor and Zahrani [7] investigated different scanning speed strategies, namely, fixed and variable scanning speeds along the straight-line to minimize variation in bending angle. Hoseinpour et al. [8] studied temperature distribution and final bending angle for square sheet of mild steel. Pitz et al. [9] presented moving mesh strategies on the laser path to reduce the simulation time. Che et al. [10] presented a study on the effects of different laser beam geometries on laser bending of sheet metal by buckling mechanism. Kyrsanidi et al. [11] presented numerical and experimental results on laser forming process of metallic plates. Lambiase [12] developed an analytical model to evaluate the bending angle in laser forming. Hu et al. [13] investigated the bending angle for Al and AISI 304 sheet metals due to laser scanning. In their following work, Hu et al. [14] studied buckling instability of laser sheet forming from measurement of bend angle for different materials and various process parameters, like sheet thickness, scanning speed, laser beam diameter and laser power, pre-bending condition, and cooling condition. Venkadeshwaran et al. [15] investigated the relationship

K. Paramasivan (✉) · S. Das · D. Misra
Jadavpur University, Kolkata, India
e-mail: parma.gce@gmail.com

between process parameters and the bending angle by using FEM and response surface methodology. They have identified the optimum value of process parameters that would increase the productivity and reduce the total operating cost and the heat-affected zone. Shen et al. [16] presented numerical and experimental investigations aimed at advancing the understanding of the edge effects in straight line laser bending process under TGM. They have used several scan strategies, namely, constant velocity, acceleration, deceleration, acceleration then deceleration, and staircase varying velocity to reduce the edge effects. Results of the study showed that the combination of acceleration and deceleration scan scheme can minimize the edge effects. Wu et al. [17] investigated laser bending of brittle materials, including mono-crystalline silicon, borosilicate glass, and Al_2O_3 ceramic. The experimental results show that bending of brittle materials occurs only when a certain temperature of specimen is achieved, so that brittle fracture could be avoided. Shi et al. [18] studied the effects of different heating methods to acquire uniform plane strain under upsetting mechanism (UM) in laser forming. Shen and Yao [19] suggested that mechanical properties (fatigue life) of the material improves after laser forming process. They have identified the residual compressive plastic strain as the most important parameter for improving the fatigue life of low carbon steel after laser forming. Hoseinpour et al. [20] investigated the statistical analysis of parameter effects on bending angle by FEM and by experiments. They have proposed the following factors which are identified to have the most significant effect on bend angle, namely, pass number, material parameter, sheet thickness, scan velocity, and beam diameter. Other factors which have less effect on bending angle are laser power and pulse duration. Liu et al. [21] performed experimental studies on stainless foil for producing negative bending angles. It is reported that buckling-mechanism-dominated laser parameters, such as larger ratio of beam diameter to specimen thickness and lower scanning speed, help to produce negative bending angles. Lambiase and Ilio [22] proposed an analytical model to predict the deformation of thin sheets (AISI 304 and AA 6013) by laser forming. Sistaninia et al. [23] introduced a new method for laser forming of plates that is laser forming with rotating and dithering beam. The result of analysis showed that the bending angle of laser beam using rotating and dithering beam in similar condition are several times more than the bending angle of laser forming using a beam which move along a straight line with uniform velocity. Lambiase et al. [24] investigated the effect of passive water cooling in laser forming of thin AISI 304 stainless steel sheets. They have reported that the cooling time and oxidation of both irradiated and cooled surfaces have been reduced by employment of passive water cooling in the laser forming of thin sheets. While at the same time, the bending angle is only marginally affected by execution of water cooling. Maji et al. [25] presented experimental investigations on pulsed laser bending of sheet metal and statistical analysis to study the effects of process parameters.

All the previous works in the area of laser forming deal with a continuous geometry. However, one often has to deal

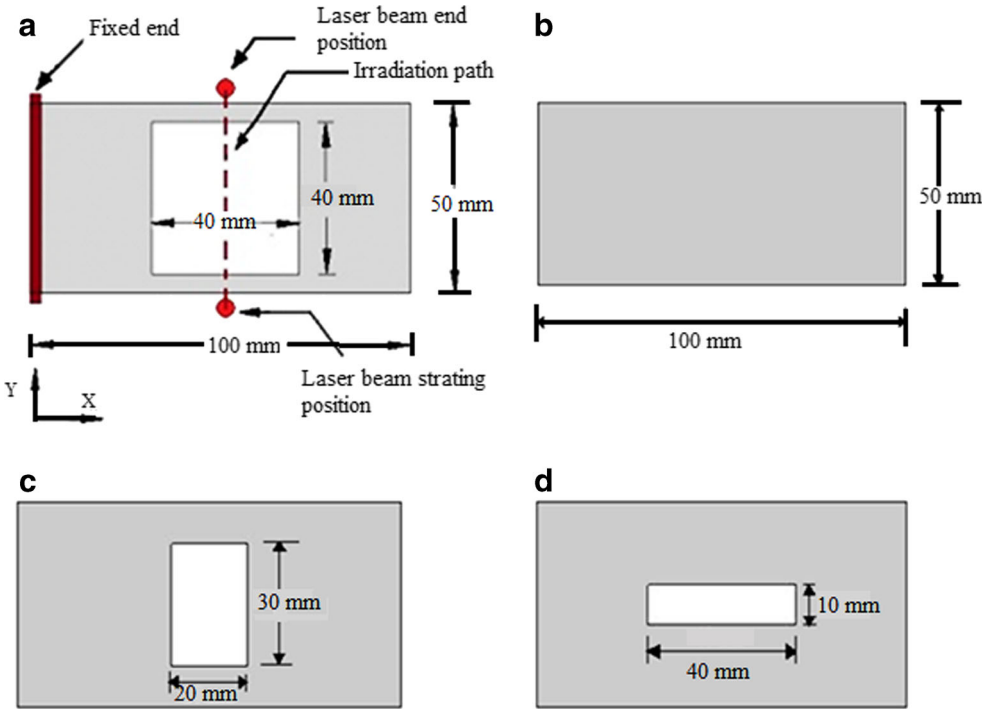

Fig. 1 Schematic diagram showing the few number of simulation work pieces and irradiation path: **a** plate with 40×40 mm^2 cut out, **b** plate without cut out, **c** plate with 20×30 mm^2 cut out, **d** plate with 40×10 mm^2 cut out

Table 1 Cutout details of the 100×50×1.5 AISI 304 plates and process parameters

Specimen conditions	Dimension of cutout ($l \times w$)	Laser power P [W]	Scanning speed V [mm/s]
Full plate ($L \times W \times T$) without cutout		250, 300, 350	10, 15, 20
Plate with cut out	10×10	250, 300, 350	10, 15, 20
	10×20		
	10×30		
	10×40		
	20×10		
	20×20		
	20×30		
	20×40		
	30×10		
	30×20		
	30×30		
	30×40		
	40×10		
	40×20		
	40×30		
	40×40		

L length of plate, W width of plate, T thickness of plate, l length of cut out, w width of cut out

with a plate with a cut out. Application of the present study will find use in automotive industries and process industries. Particularly with regard to application of the present geometry in car bodies, the front and rear panels have this type of cut out geometries requiring sheet bending. The cut outs are required for fitting bulb housings, creation of opening for mounting air grills for radiator, etc. The present work makes an attempt to study the temperature distribution and deformation on AISI 304 sheet metal with and without cut out at its center during laser beam scanning. COMSOL/MATLAB software programming code is used to develop a finite element simulation.

2 Finite element simulation

To develop a model for simulation of the laser forming process using the finite element method, following assumptions are made:

1. Material properties of the workpiece are isotropic.
2. The distribution of laser intensity follows a Gaussian mode.
3. Within the workpiece, heat transfer takes place by conduction obeying Fourier's law and heat loss by free convection and radiation are considered from the surfaces of the sheet metal to the surrounding air.
4. Melting is not involved in the workpiece during laser forming process, so phase changes and heat generation are neglected.
5. von-Mises yield criterion is considered in the bending process.

2.1 Governing equations and boundary conditions

2.1.1 Transient thermal analysis

In the present work, thermal linear elastic material model is used which combines linear elastic material with thermal expansion. During laser forming, the transient temperature field is calculated based on the mechanism of the heat

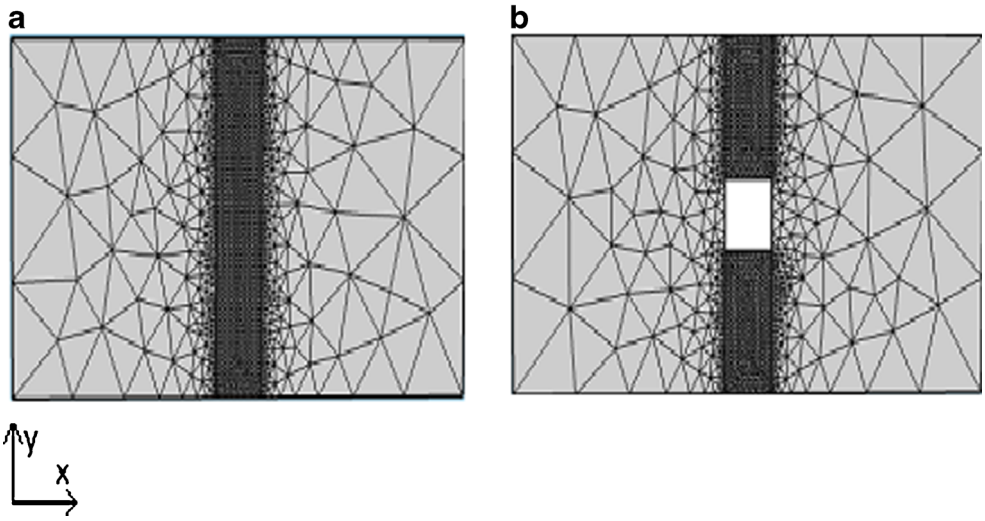

Fig. 2 Finite element meshes: **a** full plate, **b** plate with 10×10 mm^2 cut out

conduction [5]. The governing equation for heat conduction within the specimen can be written as follows:

$$\rho c\frac{\partial T(\boldsymbol{r},t)}{\partial t} = k\nabla r.(\nabla rT) \tag{1}$$

where ρ is the material density (kg/m^3), c is the specific heat (J/kg °C), k is the thermal conductivity (W/m °C), $T(\boldsymbol{r},t)$ is the temperature (K), $\boldsymbol{r}$ is the coordinate (m) in the reference configuration, t is time (s), and ∇r is the gradient operator.

The material cooling phase is made through natural convection and radiation from its surfaces exposed to ambient air. The convection boundary condition can be expressed as follows:

$$q_{\text{conv}} = h(T_s - T_0) \tag{2}$$

where, h is the heat transfer coefficient, which is taken as (10 W/m^{2}K), T_s is the sheet metal surface temperature, and T_0 is the ambient temperature, which is taken as 300 K.

The radiation boundary condition can be expressed as follows:

$$q_{\text{rad}} = \varepsilon\sigma\left(T_s^4 - T_0^4\right) \tag{3}$$

where ε is the emissivity (set as 0.6) and σ is the Stefan Boltzmann constant (5.6703×10^{-8} W/m^{2}K^4).

2.1.2 Elasto-plastic analysis

The stress equilibrium equation is given by:

$$\nabla_r\sigma(\boldsymbol{r},t) + b(\boldsymbol{r},t) = 0 \ \text{ in } \ V_r \tag{4}$$

where σ is the stress, b is the body force, and V_r is the volume of the domain (m^3). The boundary conditions is

$$u(\boldsymbol{r},t) = \overline{u}(\boldsymbol{r},t) \ \text{ on surface } A_r^u \tag{5}$$

where $\overline{u}(\boldsymbol{r},t)$ are prescribed displacements on surface A_r^u and A_r^u is surface domain (m^2).

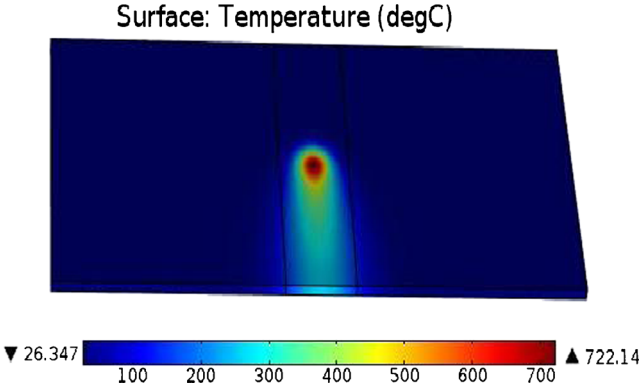

Fig. 4 Temperature distributions on the top surface at plate center (laser power=1,500 W, scanning speed=5 mm/s, spot diameter=16 mm, plate thickness=6 mm)

The total strain is the Green's strain

$$\varepsilon(\boldsymbol{r},t) = \frac{1}{2}\left[\nabla_r u(\boldsymbol{r},t) + (\nabla_r u(\boldsymbol{r},t))^T\right] \tag{6}$$

Assuming small deformation thermo-elastic-plasticity, the additive decomposition of total strain is applied as

$$\varepsilon_{\text{tot}} = \varepsilon_e + \varepsilon_p + \varepsilon_t \tag{7}$$

where, ε_{tot} is total strain, ε_e, ε_p, and ε_t are the elastic, plastic, and thermal strains, respectively.

The initial conditions are

$$u(\boldsymbol{r},t_0) = u^0(\boldsymbol{r}), \tag{8}$$

$$\varepsilon_p(\boldsymbol{r},t_0) = \varepsilon_p^0(\boldsymbol{r}), \tag{9}$$

$$\varepsilon_q(\boldsymbol{r},t_0) = \varepsilon_q^0(\boldsymbol{r}). \tag{10}$$

where ε_q is the equivalent plastic strain, and t_0 is the time for the previous time increment.

2.2 Heat flux

The moving heat flux Q produced by the laser beam is applied on the top surface of the sheet metal. In this work, laser beam

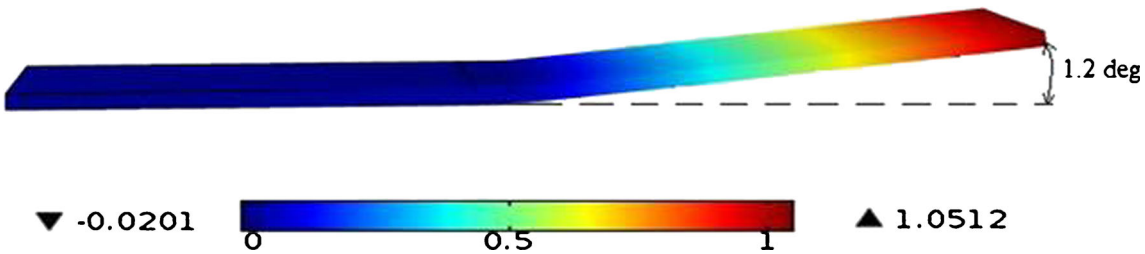

Fig. 3 z-component of displacement (mm) after single pass (laser power=375 W, scanning speed=20 mm/s, spot diameter=2 mm, plate thickness=1.5 mm)

Table 2 Validation of bending angle

Parameter				Bending angle (degrees)			Percentage error $\frac{(\varphi_p-\varphi_v)}{(\varphi_v)} \times 100$
Laser power [W]	Scanning speed [mm/s]	Spot diameter [mm]	Plate thickness [mm]	Present (φ_p)	Kyrsanidi et al. [11] (φ_v)	Venkadeshwaran et al. [15] (φ_v)	
125	20	2	1.5	0.0975	–	0.101	−3.46
375	20	2	1.5	1.2044	–	1.257	−4.18
1,500	5	16	6	0.468	0.47	–	−0.42
3,000	10	16	4	1.41	1.32	–	6.81

is assumed to have a Gaussian distribution and expressed as follows:

$$Q = \frac{2AP}{\pi R^2}\exp\left(-\frac{2r^2}{R^2}\right) \tag{11}$$

where, A is the absorption coefficient, P is the laser power [W], R is the laser beam radius (m), and r is the distance (m) of a point from the center of the laser beam.

2.3 Material properties

The material AISI 304 stainless steel is used in this numerical study. Temperature-dependent thermo-mechanical properties are used. In the model, the stress–strain behavior is expressed by bi-linear curves ranging from room temperature to high temperatures. The temperature-dependent material properties are taken from [10].

2.4 Modeling

To investigate the effect of cut out on temperature distribution and final bending angle, different dimensions of cut out are chosen in the present numerical simulation. Sixteen number of cut out plates are considered for the present study. Figure 1a shows a typical workpiece, scanning direction, and fixed end of the plate. The simply supported boundary conditions are applied at the fixed end of the plate, and the other end is free. The laser beam scanning path is at the middle of the plate along the y-axis. The process parameters used are laser power (250, 300, and 350 W), scanning speed (10, 15, and 20 mm/s), and spot diameter 2 mm. For the entire study, 1.5 mm sheet thickness is considered. The trial simulations are carried out by varying one of the process variables to find out the working range of each variables. The maximum temperature attained on the top surface is used as the criteria for choosing the working ranges, such that it neither exceeds the melting temperature nor it is too low to cause significant bending. The numerical simulation conditions are listed in Table 1. The laser beam is modeled as a moving heat flux with small time increment. Thus, a temperature distribution is obtained as a function of time. The total travel time of the laser beam is calculated based on the width of the plate and scanning speed of the laser beam. The time increment is calculated from total travel time and number of load steps.

2.5 Meshing

A 3D free tetrahedral mesh is used in this numerical modeling. To achieve better results, very fine meshes are used along the path of the laser beam. Coarse meshes are used in other parts of the plate to reduce simulation time and memory requirement. The quality of mesh element size is confirmed by a series of trial simulations increasing the mesh density until the temperatures and deformation attained saturation considering a full plate. The same mesh density is used in the scan region for all plates with cut out. The maximum length of any side of the element used is 0.000764 m in the laser path. Figure 2 shows the meshes used for plates with and without cut out.

Table 3 Validation of temperature

Parameter				Temperature at plate center (°C)		Percentage error $\frac{(\varphi_t-\varphi_s)}{(\varphi_s)} \times 100$
Laser power [W]	Scanning speed [mm/s]	Spot diameter [mm]	Plate thickness [mm]	Present (φ_t)	Kyrsanidi et al. [11] (φ_s)	
1,500	5	16	6	722	728	−0.82
3,000	10	16	4	903	844	6.99

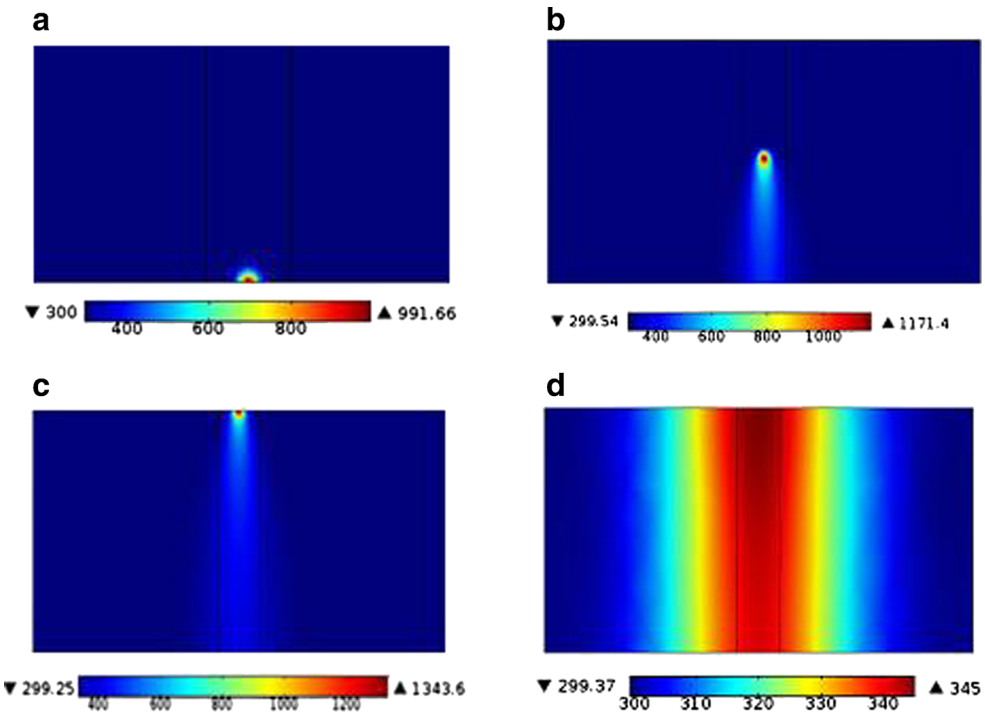

Fig. 5 Temperature distribution at four instances: **a** beam is at plate beginning (at t=0.6 s), **b** beam is at the plate center, **c** beam is at plate end, **d** after cooling (power=250 W, scanning speed=10 mm/s, plate thickness=1.5 mm, beam diameter=2 mm)

2.6 Validation of finite element model

To validate the capability of the current simulation model, the results are compared with published results of Kyrsanidi et al. [11] and Venkadeshwaran et al. [15] using ship-building steel 1.0584 (D36) and AISI 304, respectively. In the present study, we have used both the materials for validation. The plate size and process parameters are taken from their work for validation. Figure 3 shows the simulation result of z-displacement contour after single scanning pass. It is found that the results of present model is in good agreement with Venkadeshwaran et al. [15]. Two bend angles and two temperatures obtained from the simulations are compared to the experimental results reported by Kyrsanidi et al. [11]. Figure 4 shows temperature distributions on the top surface of the sheet metal at plate center. In the present model, temperature attains a maximum of 722 °C at the plate center during heating. Kyrsanidi et al. [11] have reported a maximum of 728 °C at the plate center. Tables 2 and 3 summarize the input parameters, the simulation results of bending angle and temperature, respectively. Results show that the present simulation results are in good agreement with the results from the both published results.

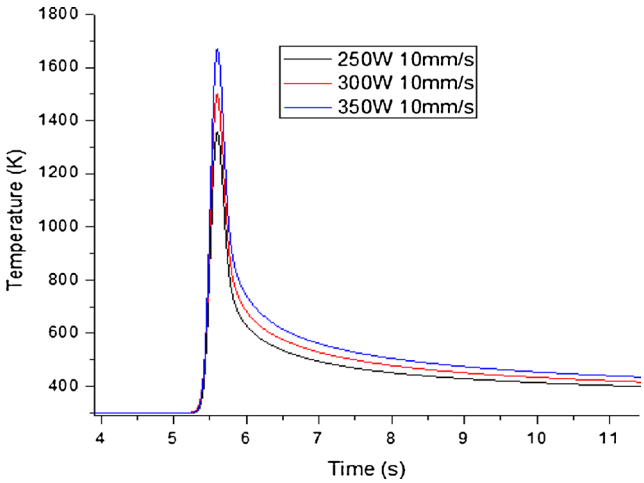

Fig. 6 Temperature history for different laser powers at top edge of the upper surface

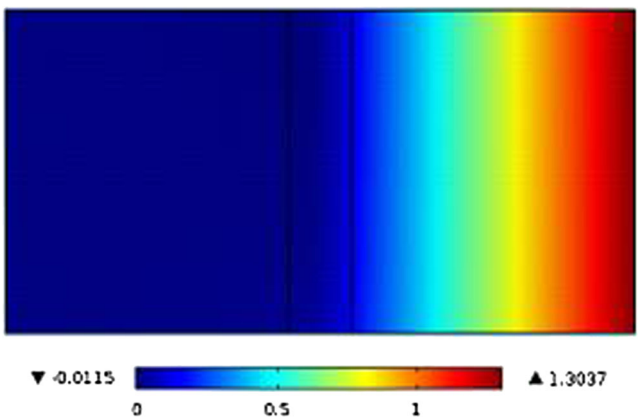

Fig. 7 z-component of displacement (mm) after cooling time (power=350 W, scanning speed=10 mm/s, plate thickness=1.5 mm, beam diameter=2 mm)

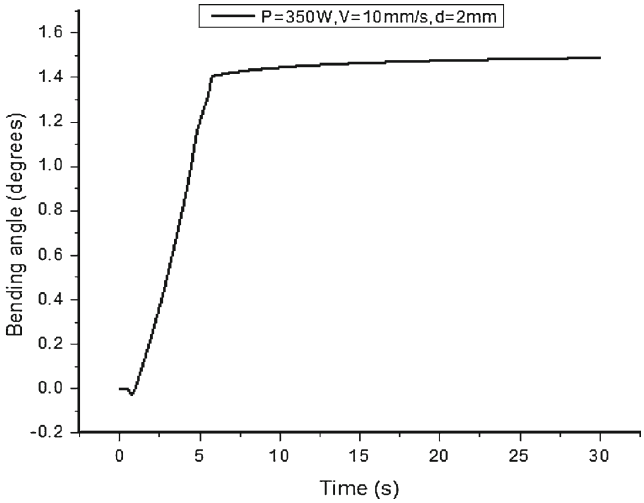

Fig. 8 Variation of bending angle with time at the top surface at a point (100, 25, and 1.5 mm)

3 Results and discussion

In the present section, effects of process parameters, namely, cut out dimensions, laser power, and scanning velocity, on thermal field and bend angle are presented for laser forming of AISI 304 plates with and without cut out.

3.1 Transient temperature and deformation fields of a rectangular plate

The plate size is taken as 100×50×1.5 mm ($L \times W \times T$). The other process parameters are laser power 250 W, velocity 10 mm/s, spot diameter 2 mm. Figure 5 shows the temperature distributions of the plate at four instances: (a) when the laser beam enters the plate (at t=0.6 s), (b) when the laser beam is at the center of the plate (at t=3.2 s), (c) when the laser beam is at the farthest edge of the plate (at t=5.6 s), and (d) after cooling (at t=30 s). It can be seen from the figures that the temperature starts rising gradually when the beam approaches the plate. Afterwards, the temperature increases rapidly until the beam leaves the plate and the temperature starts to drop. During heating, peak temperature is reached at the farthest point on the scanning line. After cooling, the temperature drops further in the range of 340 K–350 K along the midline of the plate at t=30 s.

Figure 6 shows the temperature histories of the node at the top edge of the upper surface for different laser power. Figure 7 shows the z-component of displacement on the top surface of the plate after cooling time (laser power 350 W, velocity 10 mm/s, spot diameter 2 mm). Figure 8 shows the variation of bending angle with time. It can be seen from the figure, that bending angle increases during the laser heating process and remains fixed during the cooling time. A small counter

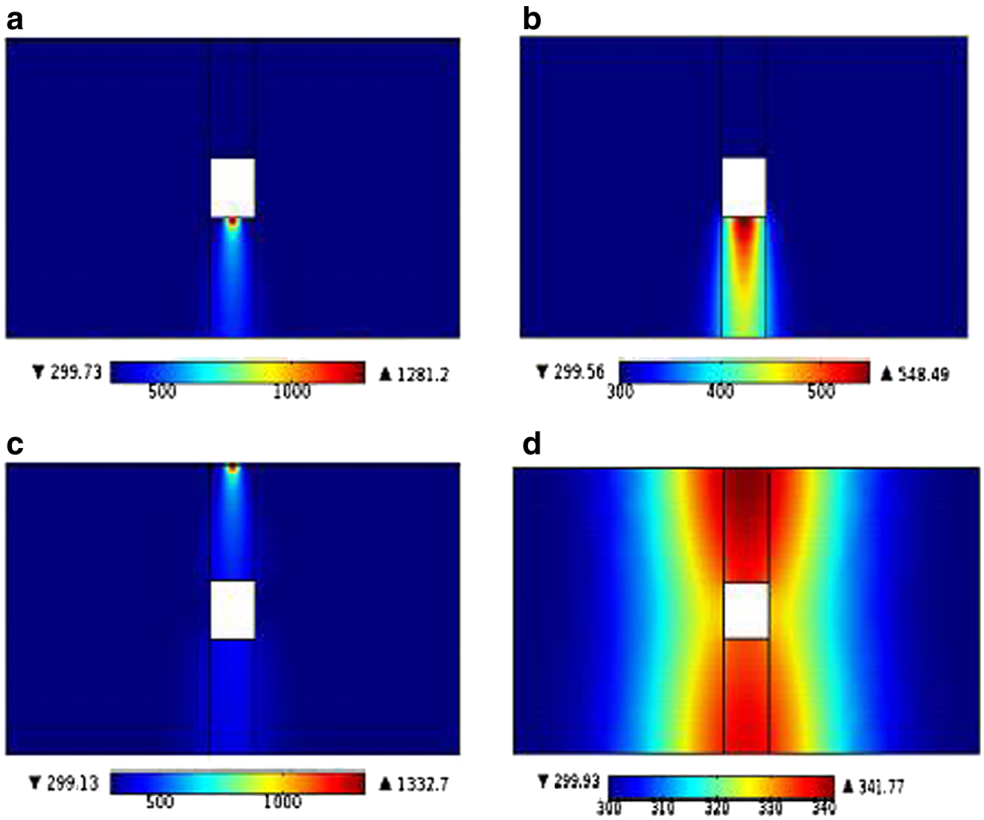

Fig. 9 Temperature distribution at four instances: **a** beam is at starting of cut out, **b** beam is inside the cut out, **c** beam is at top edge of plate, **d** after cooling (power=250 W, scanning speed= 10 mm/s, plate thickness= 1.5 mm, beam diameter=2 mm)

bending is observed until t=0.72 s, and a permanent bend angle of 1.48° is obtained at t=6 s.

3.2 Effect of cut out on transient temperature field

Figure 9 shows the temperature distributions of the cut out plate at four selected time periods: (a) when laser beam is at the start of the cut out (at t=2.6 s), (b) when laser beam has moved inside the cut out (at t=3.4 s), (c) when laser beam reaches the upper edge of the plate (at t=5.6 s), and (d) after cooling (at t=30 s). When the laser beam approaches the starting edge of the cut out, the plate temperature increases. When the laser beam enters into the cut out, the energy that had been previously delivered is dissipated rapidly to the surrounding material by conduction and the temperature falls to the range of 548 K from 1,281 K, as shown in Fig. 9a–b. During the laser heating process near the top edge of the plate the temperature rises further, and it reaches a maximum of 1,333 K as the beam leaves the top edge.

3.3 Effect of cut out on deformation field

Figure 10 shows the variation of bending angle with time at the mid-point of the free end of the plate having coordinates (100, 25, 1.5) for four different widths (w=10, 20, 30, and 40 mm) of the cut out while length of the cut out (l) is kept constant at 10 mm. It is seen that bending angle decreases with increase in width of the cut out. As a result, counter bending increases with width of cut out. When the laser beam enters the cut out, bending angle does not change. When laser beam reenters the plate through the other edge of cut out, the plate initially undergoes the same amount of counter bending, and the bending angle increases in the later part of the beam traverse. After the laser beam leaves the workpiece, a steady bending angle is obtained as evident from Fig. 10.

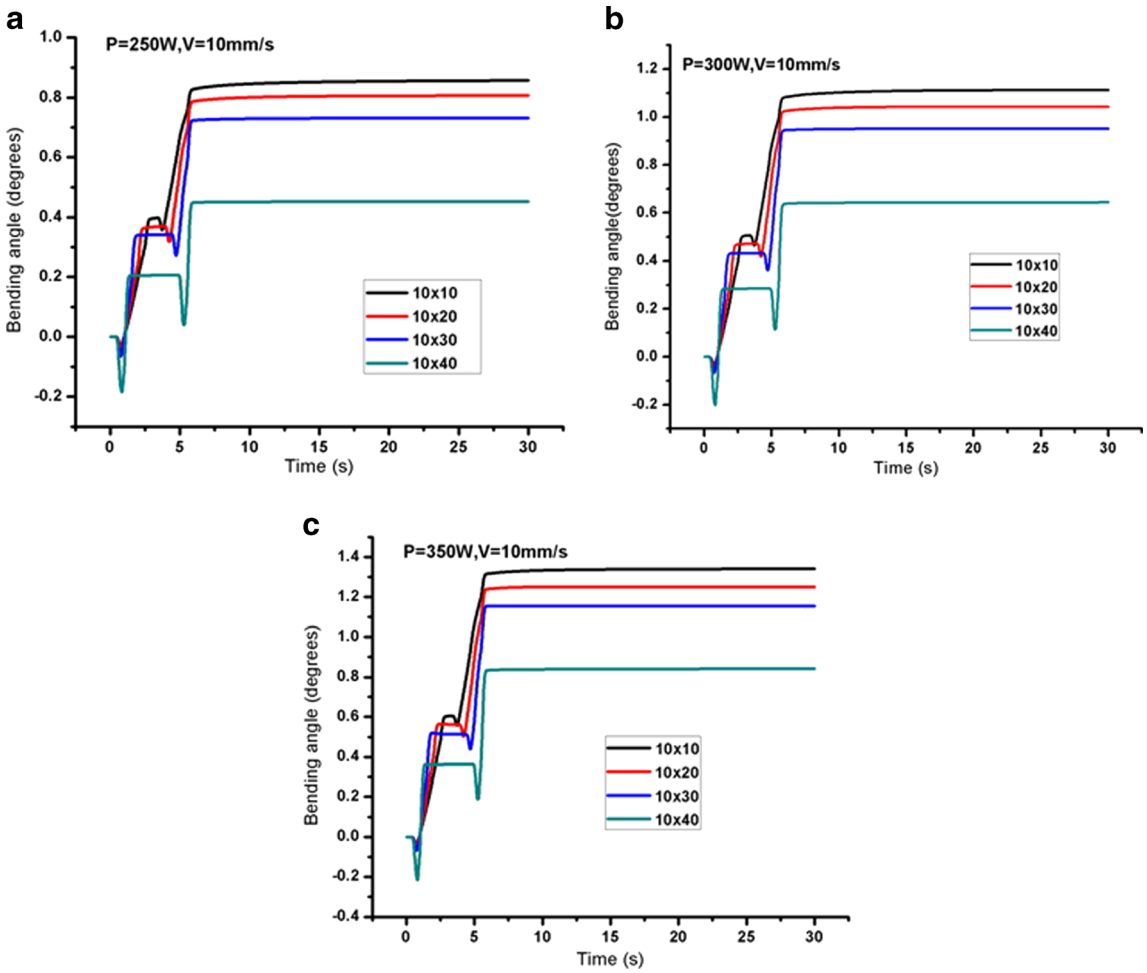

Fig. 10 Bending angle versus time for different widths (w) of cut out and laser powers: **a** power=250 W, scanning speed=10 mm/s, **b** power=300 W, scanning speed=10 mm/s, **c** power=350 W, scanning speed=10 mm/s

Figure 11 shows the variation of bending angle with time at the top surface of the plate free end at the middle having a coordinate (100, 25, 1.5) for four different widths of the cut out while length of the cut out is kept fixed at 40 mm. It can be seen that bending angle decreases with increase in width of the cut out. This is because, as the width of the cut out is more, there is lesser interaction between the laser beam and the plate material. Hence lesser energy is delivered by the laser beam and lesser energy is stored in the plate causing lesser permanent deformation (bending angle) of the plate.

Figure 12 shows the effect of changing the length of the cut out with a constant width on the bending angle under different laser powers and scanning speeds. It is observed that the variation of bending angle is very small when length of the cut out is changed from 10 to 40 mm, while the width of the cut out is kept constant at 10 mm. From the results it can be seen that as the length of the cut out is increased, keeping the width constant, there is no significant variation in bending angle.

Figure 13 shows the effect of scanning speed on bending angle at different power for different dimensions of the cut. When scanning speed increases, bending angle is reduced. As the scanning speed increases, the interaction time between the work piece and laser beam decreases, resulting in reduced absorption of heat by the work piece, resulting in lower peak temperature. Besides, the volume of the heat-affected zone is also reduced. For this reason, plastic strain as well as plastic zone also reduces. Thus, the amount of bending decreases with increase in scanning speed. From the results, it can be seen that bending angle follows a general trend of increasing magnitude with increasing power for different dimensions of the cut out. However, bending angle decreases with the increase in width of the cut out. When the width of the cut out is changed from 10 to 40 mm in y-direction while the length is kept constant at 30 mm in x-direction in Fig. 13c, the bend angle decreases from 1.32° to 0.69° for laser power of 350 W and scanning speed of 10 mm/s. The reason for this is explained earlier while discussing the effect of width of cut out.

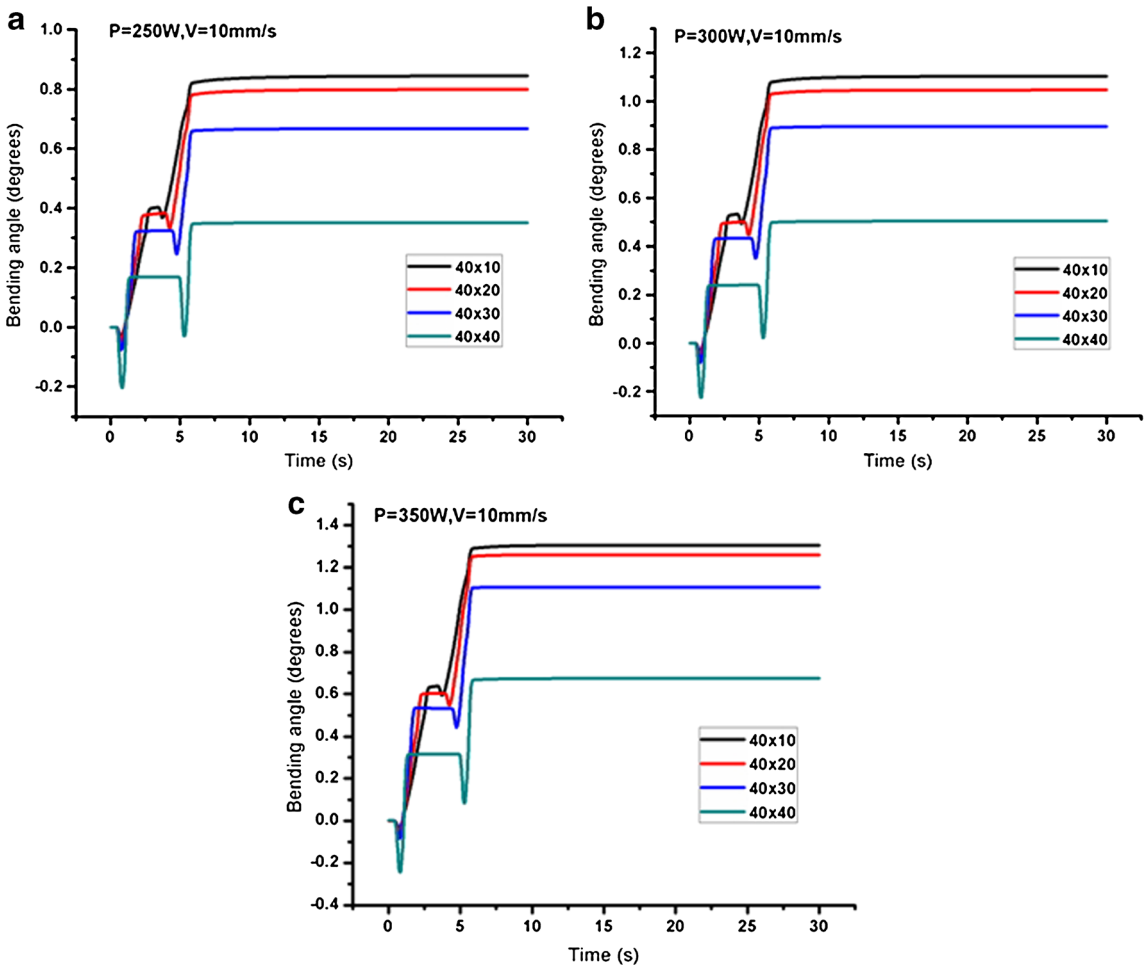

Fig. 11 Variation of bending angle versus time for different cut out widths and laser powers: **a** power=250 W, scanning speed=10 mm/s; **b** power=300 W, scanning speed=10 mm/s; **c** power=350 W, scanning speed=10 mm/s

Figure 14 shows the effect of laser power on bending angle at different scanning speeds for different dimensions of cut out. From the figure, it can be observed that bending angle increases with laser power as more energy is delivered by a higher power beam. This is because, when the laser power is increased, the peak temperature at plate and thermal stresses are increased. Therefore, the plastic strain also increases in the material. It also shows that bending angle decreases when the width of the cut out is increased from 10 to 40 mm in *y*-direction while length of the cut out is kept constant at 20 mm in *x*-direction.

3.4 Effect of cutout at different location on plate

To investigate effect of cutout at different position in the plate, the same dimension of the cutout is used in this study. Eight numbers of cutout plates and one full plate (without cut out)

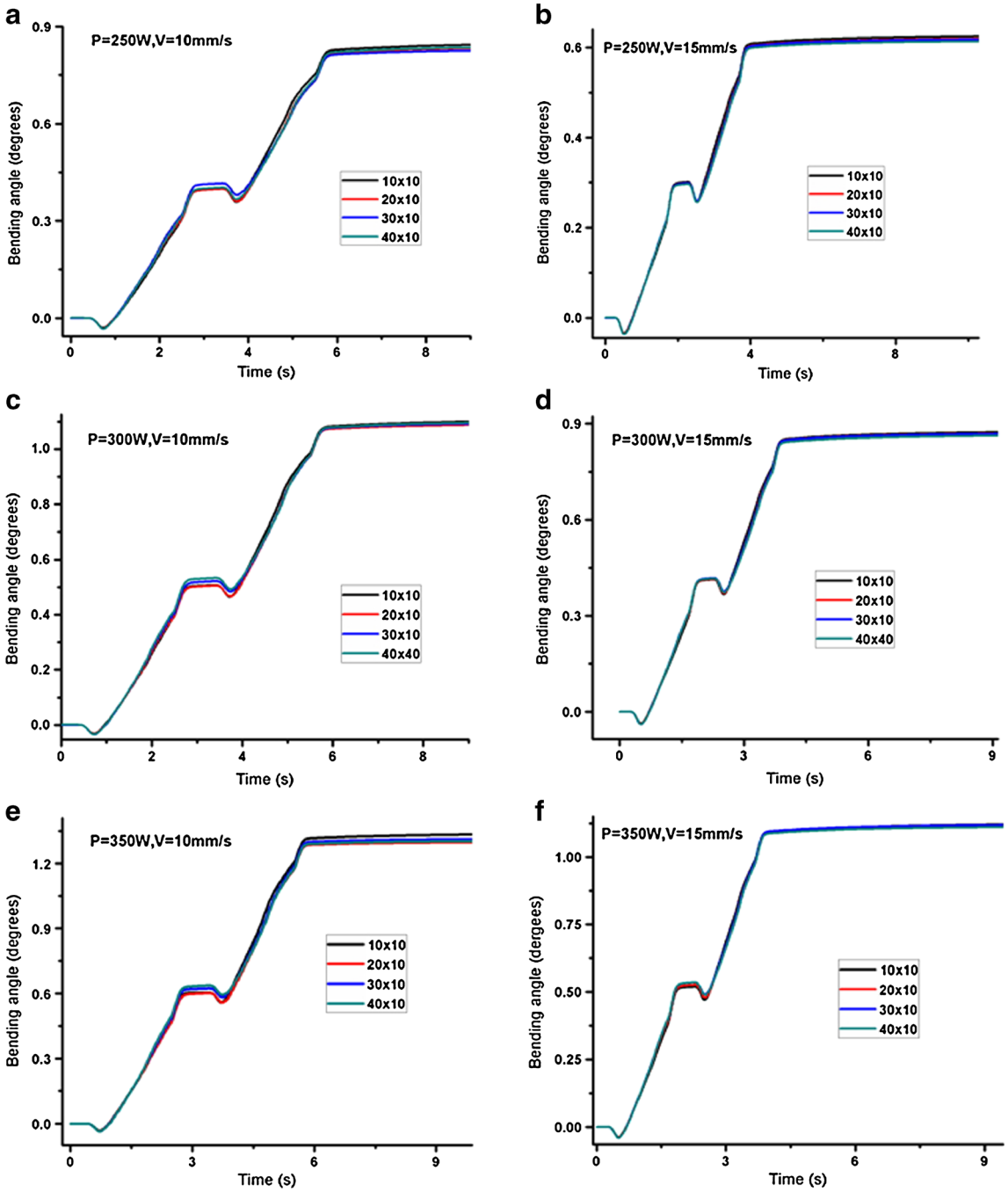

Fig. 12 Variation of bending angle with time for different laser powers and cut out dimensions

are considered. All workpieces have the same length (100 mm), width (50 mm), and thickness (1.5 mm). The cutout dimension is taken as 10×10 mm^2 (length×width). The other process parameters are: laser power 250 W, velocity 10 mm/s, and spot diameter 2 mm. The cutout position is varied along the scanning path and outside of the scanning path as well.

Figure 15a shows the effect of changing the position of the cut out along the scanning path, on bending angle under identical process conditions. Three numbers of cutout plates are considered. The cut out width is placed at different y with the coordinates of the left-bottom point of the cut out at x=45 mm and y=10, 20, and 30 mm. It is observed that bending angle does not get affected by changing the position of the cut out along the scanning path. The full plate undergoes higher bending than the cut out plates. Heat transfer on the surface is reduced because of lesser interaction time for samples with cutout in comparison to that of a full plate. Therefore, less bending angle is achieved in a plate with cut out than that in a full plate under the same process conditions.

Figure 15b shows the effect of changing the position of the cut out in x-direction on bending angle. Five numbers of cutout plates are considered for this study. The cutout is placed at different x with the left-bottom point of the cut out at x=10, 30, 45, 60, and 80 mm and y=20 mm. It shows that bending angle does not vary significantly when the position of the cut out is changed along the x-direction. Out of all the plates, the plate with cutout at x=45 mm has got minimum bending angle because in this case the cutout is placed in the path of laser scanning, reducing the interaction time.

4 Conclusion

The aim of this numerical study is to identify the effects of process parameters on temperature distribution and final bending angle of AISI 304 stainless steel sheet. In addition, the effect of a rectangular cut out at the middle of the sheet is also investigated. A three-dimensional numerical simulation is performed by selecting different laser powers, scanning

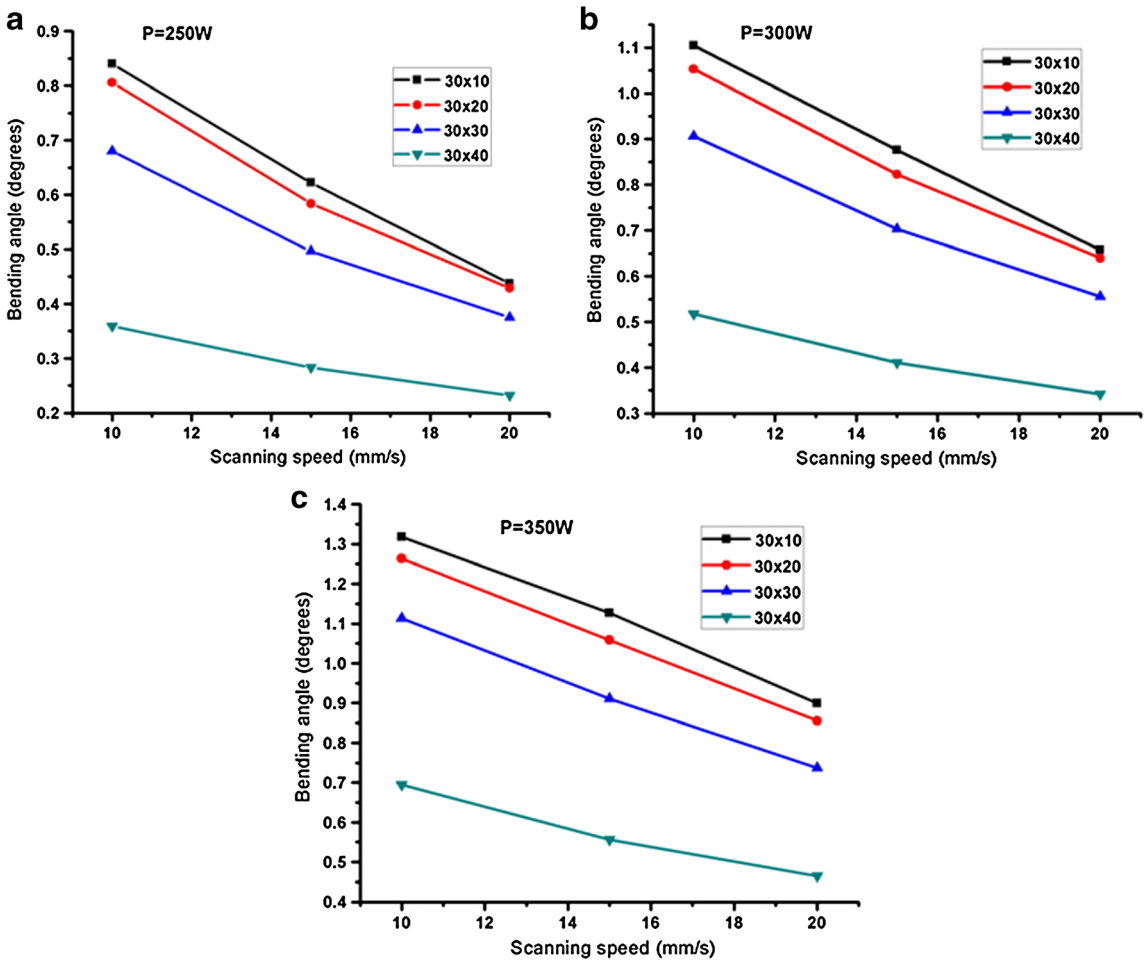

Fig. 13 Effect of scanning speed on bending angle at different power for different process parameter: **a** power=250 W, **b** power=300 W, **c** power=350 W

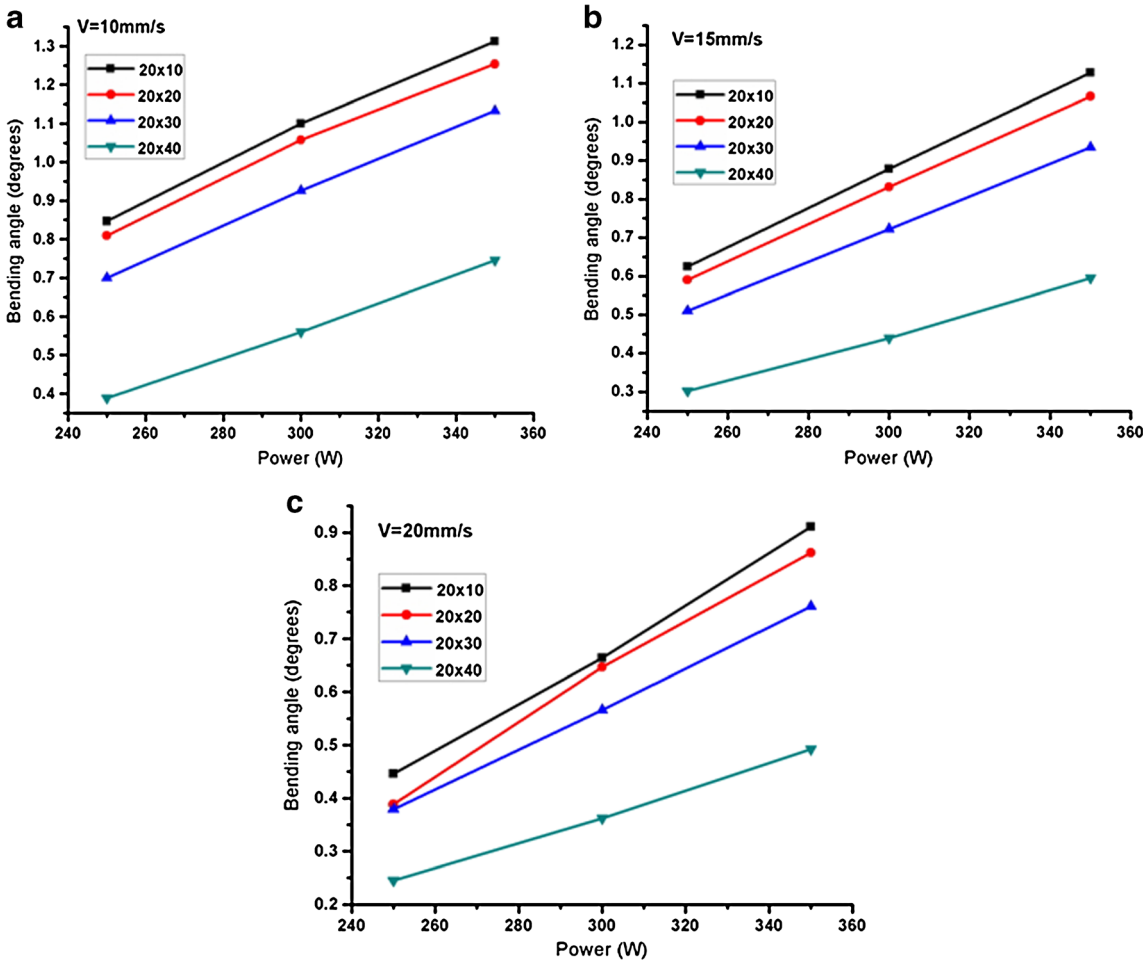

Fig. 14 Effect of laser power on bending angle at different scanning speed for different process parameters: **a** scanning speed=10 mm/s, **b** scanning speed=15 mm/s, **c** scanning speed=20 mm/s

speeds, and dimensions of the cut out. Bending angle, temperature distribution, residual stresses, and plastic strains are obtained from the numerical simulations. From the results of numerical simulation, it is seen that laser power, scanning speed, and dimensions of the rectangular cut out play important roles in the laser forming process and the final bending angle. Bending angle increases with laser power and decreases with increasing scanning speed. Bending angle is also affected

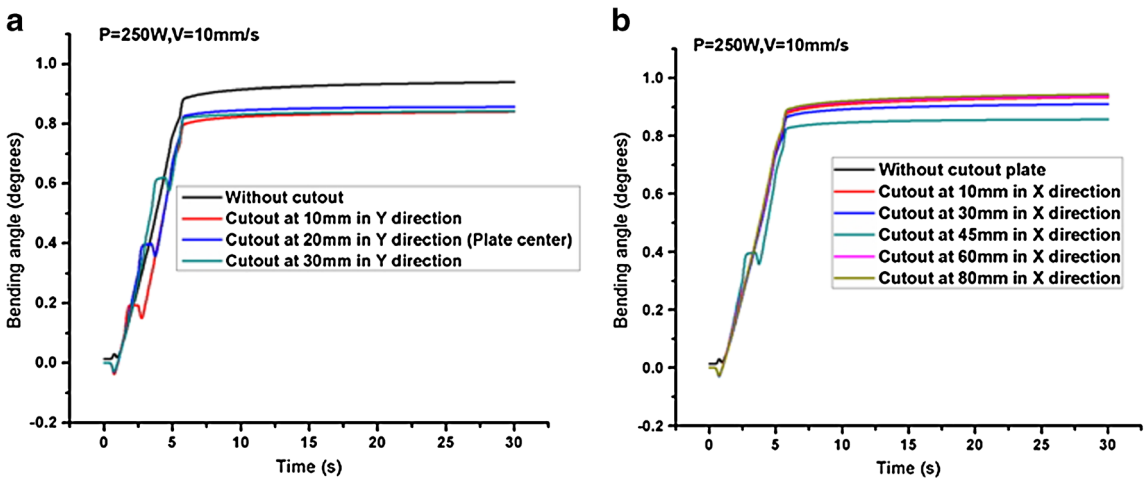

Fig. 15 Effect of cutout location on bending angle for same process parameter: **a** varying position of cutout along scanning path (*y* direction), **b** varying position of cutout in *x* direction

by varying the width of the cut out in laser scanning path with the same process parameters. It decreases with increase in width of the cut out. This is caused due to the reduced interaction time between the work piece and the laser beam. Effect of length of the cut out and position of cut out along the scanning path have no significant effect on the final bending angle.

References

1. Shen H, Vollertsen F (2009) Modelling of laser forming—an review. Comput Mater Sci 48:834–840
2. Ji Z, Wu S (1998) FEM simulation of the temperature field during the laser forming of sheet metal. J Mater Process Technol 74:89–95
3. Wu S, Ji Z (2002) FEM simulation of the deformation field during the laser forming of sheet metal. J Mater Process Technol 121:269–272
4. Shi YJ, Shen H, Yao ZQ, Hu J (2006) Numerical investigation of straight-line laser forming under the temperature gradient mechanism. Acta Metall Sin (English Letters) 19(2):144–150
5. Venkadeshwaran K, Das S, Misra D (2010) Finite element simulation of 3-D laser forming by discrete section circle line heating. Int J Eng Sci Technol 2(4):163–175
6. Yu G, Masubuchi K, Maekawa T, Patrikalakis NM (2001) FEM simulation of laser forming of metal plates. J Manuf Sci Eng 123: 405–410
7. Zohoor M, Zahrani EG (2012) Experimental and numerical analysis of bending angle variation and longitudinal distortion in laser forming process. Scientia Iranica 19:1074–1080
8. Hoseinpour Gollo M, Moslemi Naeini H, Mostafa Arab NB (2011) Experimental and numerical investigation on laser bending process. J Comput Appl Res Mech Eng 1(1):45–52
9. Pitz I, Otto A, Schmidt M (2010) Simulation of the laser beam forming process with moving meshes for large aluminium plates. Phys Procedia 5:363–369
10. Che J, Sheikh M, Li L (2011) A study of the effect of laser beam geometries on laser bending of sheet metal by buckling mechanism. Opt Laser Technol 43:183–193
11. Kyrsanidi AK, Kermanidis TB, Pantelakis SG (1999) Numerical and experimental investigation of the laser forming process. J Mater Process Technol 87:281–290
12. Lambiase F (2012) An analytical model for evaluation of bending angle in laser forming of metal sheets. J Mater Eng Perform 21:2044–2052
13. Hu Z, Labudovic M, Wang H, Kovacevic R (2001) Computer simulation and experimental investigation of sheet metal bending using laser beam scanning. Int J Mach Tools Manuf 41:589–607
14. Hu Z, Kovacevic R, Labudovic M (2002) Experimental and numerical modeling of buckling instability of laser sheet forming. Int J Mach Tools Manuf 42:1427–1439
15. Venkadeshwaran K, Das S, Misra D (2012) Bend angle prediction and parameter optimisation for laser bending of stainless steel using FEM and RSM. Int J Mechatron Manuf Syst 5(3–4):308
16. Shen H, Hu J, Yao Z (2010) Analysis and control of edge effects in laser bending. Opt Lasers Eng 48(3):305–315
17. Wu D, Zhang Q, Ma G, Guo Y, Guo D (2010) Laser bending of brittle materials. Opt Lasers Eng 48(4):405–410
18. Shi Y, Liu Y, Yi P, Hu J (2012) Effect of different heating methods on deformation of metal plate under upsetting mechanism in laser forming. Optics Laser Technol 44(2):486–491
19. Shen H, Yao Z (2009) Study on mechanical properties after laser forming. Opt Lasers Eng 47(1):111–117
20. Hoseinpour Gollo M, Mahdavian SM, Moslemi Naeini H (2011) Statistical analysis of parameter effects on bending angle in laser forming process by pulsed Nd:YAG laser. Optics Laser Technol 43(3):475–482
21. Liu J, Sun S, Guan Y, Ji Z (2010) Experimental study on negative laser bending process of steel foils. Opt Lasers Eng 48(1):83–88
22. Lambiase F, Ilio A (2013) A closed-form solution for thermal and deformation fields in laser bending process of different materials. Int J Adv Manuf Technol 69:849–861
23. Sistaninia M, Sistaninia M, Moeanodini H (2009) Laser forming of plates using rotating and dithering beams. Comput Mater Sci 45(2): 480–488
24. Lambiase F, Ilio A, Paoletti A (2012) An experimental investigation on passive water cooling in laser forming process. Int J Adv Manuf Technol 64:829–840
25. Maji K, Pratihar D, Nath AK (2013) Experimental investigations and statistical analysis of pulsed laser bending of AISI304 stainless steel sheet. Opt Laser Technol 49:18–27